

# A comparison between the photophysical and photosensitising properties of tetraphenyl porphycenes and porphyrins

Noemí Rubio,<sup>a</sup> Ferran Prat,<sup>a</sup> Núria Bou,<sup>a</sup> José I. Borrell,<sup>a</sup> Jordi Teixidó,<sup>a</sup> Ángeles Villanueva,<sup>b</sup> Ángeles Juarraz,<sup>b</sup> Magdalena Cañete,<sup>b</sup> Juan C. Stockert<sup>b</sup> and Santi Nonell<sup>\*a</sup>

<sup>a</sup> Grup d'Enginyeria Molecular, Institut Químic de Sarrià, Universitat Ramon Llull, Via Augusta 390, 08017 Barcelona, Spain. E-mail: s.nonell@iqs.es; Fax: +34-93-205-62-66; Tel: +34-93-267-20-00

<sup>b</sup> Departamento de Biología, Facultad de Ciencias, Universidad Autónoma de Madrid, 28049 Madrid, Spain

Received (in Durham, UK) 4th October 2004, Accepted 13th December 2004  
First published as an Advance Article on the web 12th January 2005

The photophysical properties of 2,7,12,17-tetraphenylporphycene (TPPo) and its palladium(II) (PdTPPo) and copper(II) (CuTPPo) complexes as well as comparisons with those of their porphyrin counterparts are reported. All porphycenes absorb in the red part of the spectrum, but only TPPo shows fluorescence ( $\Phi_F = 0.15$ ). This compound presents good quantum yields of triplet ( $\Phi_T = 0.33$ ) and singlet oxygen ( $\Phi_\Delta = 0.23$ ) formation. In the case of PdTPPo, fluorescence is inhibited by the internal heavy-atom effect and the triplet and singlet oxygen quantum yields are enhanced ( $\Phi_T = \Phi_\Delta = 0.78$ ). The presence of the paramagnetic ion Cu(II) in CuTPPo further enhances the non-radiative transitions leading to an internal conversion quantum yield  $\Phi_{ic} = 0.65$  and to a triplet quantum yield  $\Phi_T = 0.35$ . With a triplet lifetime of 700 ns, CuTPPo is nevertheless able to sensitise singlet oxygen with a quantum yield that strongly depends on the oxygen concentration in the environment. These photophysical properties, together with their ability to kill several cancer cell lines, place these sensitisers in a good position to be used in photodynamic therapy (PDT).

## 1. Introduction

In 1986, Vogel<sup>1</sup> synthesised a new tetrapyrrolic isomer of porphyrin, called porphycene, obtained by reshuffling of the pyrrole and methine moieties of the porphyrin structure. Owing to the change of symmetry, this structural isomer showed higher absorption intensity than porphyrins in the spectral region above 630 nm, where the tissue is more transparent to light,<sup>2</sup> thus placing porphycenes in a good position as potential candidates for photodynamic therapy (PDT). In fact, studies of cell photoinactivation have demonstrated their usefulness as PDT photosensitisers.<sup>3–12</sup> The absorption in the red part of the spectrum can be modulated by substitution on the porphycene ring in a way where both the substituent nature and its position have a synergic effect. Thus, 9,10,19,20-tetra-alkyl substitution leads to a bathochromic shift of 30–50 nm with respect to the non-substituted porphycene<sup>13</sup> whereas alkyl-substitution at the 2,7,12,17-positions causes a more minor effect.<sup>14</sup>

Similar to porphyrins<sup>15,16</sup> and other porphyrin isomers,<sup>17</sup> porphycenes are able to form metallic complexes called metalloporphycenes. However this ability is, except for small cations, somewhat lower than that of porphyrins because their inner cavity is smaller and slightly rectangular and the electron lone pairs are not oriented towards the centre of the molecule to facilitate the entrance of the metallic cation. Nevertheless, the size and shape of the inner cavity can be modulated to some extent—and therefore facilitates the metallic complexation of the free base—by choosing the position where the substituents are introduced.<sup>13</sup> Thus, several metalloporphycenes—such as 2,7,12,17-tetrapropylporphycenato nickel(II),<sup>18–20</sup> 2,7,12,17-tetrapropylporphycenato palladium(II) and -platinum(II),<sup>19</sup> 9,10,19,20-tetrapropylporphycenato nickel(II),<sup>13,21</sup> octaethyl-

porphycenato zinc(II),<sup>22,23</sup> pyridine(octaethylporphycenato) zinc(II) and etioporphycenato zinc(II),<sup>22</sup> octaethylporphycenato nickel(II), cobalt(II), copper(II) and octaethylporphycenato chloroiron(III), and chloromanganese(II)<sup>23</sup>—have been synthesised and in some cases their photophysical properties have been determined.

All the compounds above are alkyl-substituted porphycenes. Since aryl-substitution is synthetically available, a comparison of the photophysical properties of aryl-substituted porphycenes to both the alkyl-substituted counterparts as well as to aryl-substituted porphyrins is of interest for the development of porphycene-based PDT photosensitisers. Such comparative studies are reported in this work for 2,7,12,17-tetraphenylporphycene (TPPo) and its palladium(II) (PdTPPo) and copper(II) (CuTPPo) complexes (Fig. 1).

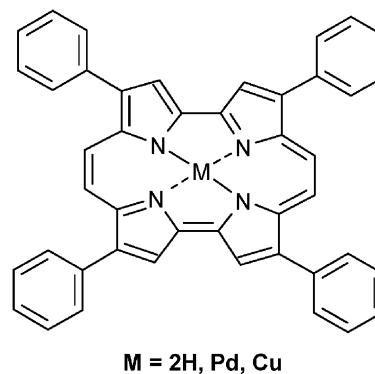


**Fig. 1** Structure of 2,7,12,17-tetraphenylporphycene (TPPo) and its Pd(II) and Cu(II) complexes.

## 2. Materials and methods

### Chemicals

TPPo and PdTPPo were synthesised as described previously.<sup>11,24,25</sup> CuTPPo was synthesised following the same procedure as for PdTPPo. 2,7,12,17-Tetra-*n*-propylporphycene (TPrPo) was a kind gift from Professor Silvia E. Braslavsky from the Max-Planck-Institut für Strahlenchemie. Benzophenone (BP) (>99%), 2-hydroxybenzophenone (2-HBP) (99%), mesoporphyrin dimethyl ester (MPDME) (98%), zinc(II)-5,10,15,20-tetraphenylporphine (ZnTPP), phenalenone (PN) (97%), 1-iodopropane (99%) and benzonitrile (99.9%, HPLC grade) were all purchased from Aldrich and used as received. Tetrabutylammonium perchlorate electrochemical grade was purchased from Fluka. Toluene, benzene, methanol, acetone and dichloromethane were of spectroscopic grade (Panreac). Acetonitrile was of HPLC grade (SDS). For the cyclic voltammetry experiments, dimethylformamide (DMF) >99.8% pure and dichloromethane >99.95% pure were purchased from SDS and were dried over activated molecular sieves 4 Å from Merck. Argon 5.0 was from Abelló-Linde and helium and oxygen from Air-Liquide N-50.

### Photophysical measurements

Unless stated otherwise, all measurements were carried out in toluene. The porphycenes described are not soluble in water. Absorption spectra were recorded on a Varian Cary 4 spectrophotometer. Fluorescence spectra were recorded with two spectrofluorimeters: for general studies a Hitachi HF-4500 with 2.5 mm slits for both excitation and emission was used and a SPEX Fluorolog with 2.5 mm slits was used for fluorescence quantum yield ( $\Phi_F$ ) determinations. The latter were assessed by comparing the areas under the emission curves of a series of optically-matched solutions of the samples and the references. The substance used as the reference was TPrPo ( $\Phi_F = 0.38 \pm 0.06$ , in toluene).<sup>26</sup> The singlet lifetime was determined by time-correlated single photon counting using a fluorescence lifetime system (PicoQuant Fluotime 200) equipped with a red-sensitive photomultiplier tube. A laser diode emitting at 375 nm, 10 MHz repetition rate, was used for excitation, and the detector count rate was always kept below 2 KHz. The singlet energy was estimated from the intersection point of the normalised absorption and fluorescence spectra.

The triplet energy was determined from near-IR phosphorescence studies. Samples in 1-iodopropane were either air-saturated or degassed through several pump-thaw-freeze cycles. Excitation was produced by a 1000 W Hg-Xe lamp filtered using 10 cm water, a cut-off filter at 510 nm, and finally an additional Schott KG5 filter. Near-IR luminescence was detected with a North Coast EO-817L germanium photodiode. The triplet energy was determined at 90% of the maximum peak height assuming a similar Stokes shift as in the fluorescence spectrum.

The triplet quantum yield was determined by laser-induced optoacoustic calorimetry (LIOAC) on argon-saturated solutions, using a ceramic piezoelectric transducer to sense the pressure wave induced by the non-radiative relaxation events leading to the production of the triplet state.<sup>27</sup> With the aid of a calorimetric reference that releases all the absorbed energy as heat (2-HBP), the energy stored in the photoproduced triplets,  $\Phi_T \cdot E_T$ , could be readily determined by comparing the maximum amplitude of the optoacoustic waves for a series of solutions containing variable amounts of the sensitizer irradiated under the same conditions. Specifically, the maximum amplitude of the LIOAC waves was plotted against the absorption factor  $1-10^{-A}$ , where  $A$  is the absorbance at the excitation wavelength. Assuming no significant structural-

volume changes between the triplet and the ground state, the slope of the linear plot obtained is proportional to the heat released within the time resolution of the experiment, *ca.* 10 ns. This accounts for the heat released upon relaxation of the Franck-Condon state to the relaxed singlet state and subsequent formation of the triplet state. The ratio of slopes between the sensitizer and the calorimetric reference,  $\phi$ , can thus be equated to  $\phi = 1 - (\Phi_F \cdot E_F/E_{exc}) - (\Phi_T E_T/E_{exc})$  where  $E_F$  is the average energy of the fluorescence photons and  $E_{exc}$  is the energy of the laser photons. In our case the excitation source was a nitrogen laser (337 nm,  $E_{exc} = 356 \text{ kJ mol}^{-1}$ , 6 ns pulsewidth, 10–100  $\mu\text{J pulse}^{-1}$ ; Radiant Dyes Accessories GmbH RDN 50/25).

The triplet lifetime, triplet-minus-singlet spectrum and rate constant for quenching by oxygen were determined by nanosecond laser flash photolysis. Two different systems were used: the first one was a LKS 50 system from Applied Photophysics. The second one was a home-built system made up of an OPO laser (SL OPO, Continuum; 5 ns pulsewidth, 1–10 mJ pulse<sup>-1</sup>) pumped by a Q-switched Nd-YAG laser (Surelite I-10, Continuum) and photoinduced absorbance changes were monitored at 90 degrees by an analyzing beam produced by a Xe lamp (PTI, 75 W) in combination with a dual-grating monochromator (mod. 101, PTI) coupled to a photomultiplier (Hamamatsu R928) for 300–800 nm detection and a North Coast EO-817P germanium detector for 800–1600 nm. The triplet-minus-singlet absorption coefficients were determined by the comparative method of Bensasson *et al.*<sup>28</sup> using BP ( $\Delta\epsilon_{T-S} = 7200 \text{ M}^{-1} \text{ cm}^{-1}$  at 535 nm,  $\Phi_T = 1.0$ ),<sup>29</sup> MPDME ( $\Delta\epsilon_{T-S} = 27000 \text{ M}^{-1} \text{ cm}^{-1}$  at 440 nm,  $\Phi_T = 0.81$ )<sup>30</sup> or ZnTPP ( $\Delta\epsilon_{T-S} = 74000 \text{ M}^{-1} \text{ cm}^{-1}$  at 470 nm,  $\Phi_T = 0.88$ )<sup>31</sup> as standards in toluene. The rate constant for oxygen quenching was determined from Stern-Volmer analysis of the triplet lifetime in argon-, air- and oxygen-saturated solutions.

The quantum yield for singlet oxygen ( $\text{O}_2(^1\Delta_g)$ ) production ( $\Phi_\Delta$ ) and the rate constant for its quenching by the sensitizer were determined by time-resolved near-IR spectroscopy (TRNIR). The luminescence from samples excited by 337 nm pulses from the N<sub>2</sub> laser was filtered through a cut-off silicon filter (Glenn-Creston;  $\lambda > 1050 \text{ nm}$ ) and an interference filter at 1270 nm (Spectrogon). Detection of the weak  $\text{O}_2(^1\Delta_g)$  phosphorescence was achieved with a germanium photodiode (Judson J16 8Sp) and amplified with a home-built preamplifier and a Comlinear amplifier (LHE 103 A, gain = 10). Signal averaging was performed to improve the signal-noise ratio. The quantum yield was deduced from the signal intensity by a comparative method<sup>32</sup> using PN as standard ( $\Phi_\Delta = 0.92$  in toluene).<sup>33,34</sup> The quenching rate constant was calculated from Stern-Volmer analysis of the observed decay rate constant for  $\text{O}_2(^1\Delta_g)$  in dichloromethane.

The oxidation and reduction potentials were determined by cyclic voltammetry with two different systems. The first one used a cylindrical cell with a 0.093 cm<sup>2</sup> platinum sphere as the work electrode, a platinum wire as the counter-electrode, and an SCE as the reference electrode. The second system employed a spherical cell with a 1 cm<sup>2</sup> platinum foil as the work electrode, a platinum wire as the counter electrode, and Ag/AgCl as the reference electrode. The voltammograms were recorded in argon-saturated dried methylene chloride or DMF using tetrabutylammonium perchlorate as a supporting electrolyte, with sweep speeds ranging from 20 to 200 mV s<sup>-1</sup>.

## 3. Results and discussion

The photophysical and electrochemical properties of the three tetraphenylporphycenes studied are discussed in detail in the following sections. A summary is given in Table 1.

**Table 1** Summary of the photophysical properties (in toluene) of the porphycenes studied

	TPPo	PdTPPo	CuTPPo
$\lambda_{\text{max}}/\text{nm}$	659	632	644
$\log(\epsilon_{\text{S}}/\text{M}^{-1}\text{cm}^{-1})$	4.7	4.9	4.8
$E_{\text{S}}/\text{kJ mol}^{-1}$	181	188	182
$\Phi_{\text{F}}$	0.15	$<10^{-4}$	$<10^{-4}$
$\tau_{\text{S}}(\text{air})/\text{ns}$	4.8	—	—
$E_{\text{T}}/\text{kJ mol}^{-1}$	124	126	126
$\Phi_{\text{T}}$	0.33	0.78	0.35
$\Phi_{\text{ic}}$	0.52	0.22	0.65
$\tau_{\text{T}}(\text{Ar})/\mu\text{s}$	51	4.4	0.7
$k_{\text{q}}^{\text{O}_2}/10^9\text{ M}^{-1}\text{s}^{-1}$	2.9	1.8	2.0
$\Phi_{\Delta}$	0.23	0.78	0.24 <sup>a</sup>
$k_{\text{q}}^{\text{S}}/10^7\text{ M}^{-1}\text{s}^{-1}$	4.4	3.2	$<10$

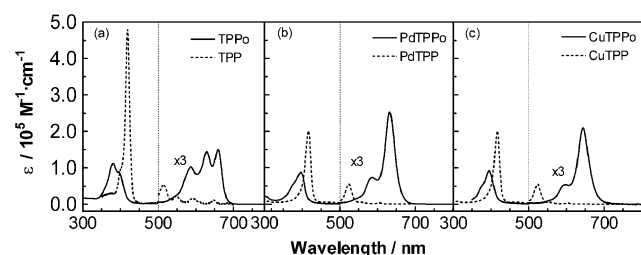
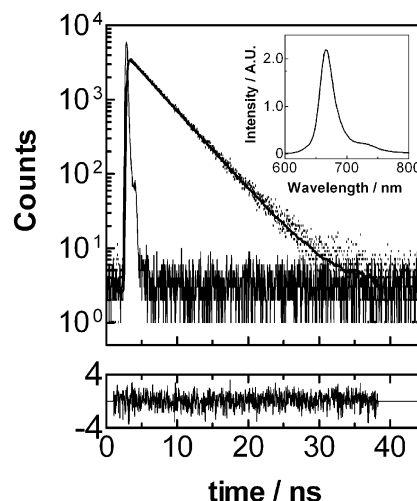
$\lambda_{\text{max}}$ , maximum of the lowest-energy absorption band;  $\epsilon_{\text{S}}$ , absorption coefficient at  $\lambda_{\text{max}}$ ;  $E_{\text{S}}$ , energy of the singlet state;  $\Phi_{\text{F}}$ , quantum yield of fluorescence;  $\tau_{\text{S}}$ , lifetime of the singlet state;  $E_{\text{T}}$ , energy of the triplet state;  $\Phi_{\text{T}}$ , quantum yield of triplet formation;  $\tau_{\text{T}}$ , lifetime of the triplet state;  $k_{\text{q}}^{\text{O}_2}$  rate constant for triplet quenching by ground-state oxygen;  $\Phi_{\Delta}$ , quantum yield of singlet oxygen formation;  $k_{\text{q}}^{\text{S}}$  rate constant for singlet oxygen quenching by the sensitizer.<sup>a</sup> In air. See text.

### Free-base porphycene

Similar to other pyrrole-based macrocycles, the spectrum of TPPo shows an intense Soret band around 378 nm and three Q-bands at 586, 628 and 659 nm. The latter is red shifted *ca.* 30 nm relative to porphycene (Po) and 2,7,12,17-tetra-*n*-propylporphycene (TPrPo).<sup>14</sup> Compared to its porphyrin counterpart 5,10,15,20-tetraphenylporphyrin (TPP), the lowest-energy Q-band is 11 nm red-shifted and one order of magnitude more intense, whereas the Soret band is 41 nm blue-shifted and *ca.* 3 times less intense (Fig. 2). The position and intensity of the Q-bands confer porphycenes an advantage for PDT applications relative to porphyrins,<sup>2</sup> requiring lower doses of drug and light to produce the same concentration of excited states.

TPPo shows fluorescence with a maximum at 667 nm and with quantum yield  $\Phi_{\text{F}} = 0.15 \pm 0.03$  in argon-saturated solutions (Fig. 3 inset). While this value is substantially lower than that of TPrPo ( $\Phi_{\text{F}} = 0.38 \pm 0.06$ ),<sup>26</sup> it is still comparable to that of TPP ( $\Phi_{\text{F}} = 0.13$ )<sup>31,35</sup> and other porphyrins used as tumour markers such as haematoporphyrin derivative (HpD) ( $\Phi_{\text{F}} \approx 0.09$ ).<sup>36</sup> Thus, TPPo clearly appears as a potential agent for tumour diagnosis.

The fluorescence decay of TPPo could be fitted to a single exponential decay model. The singlet lifetime is 4.8 ns, much shorter than that of TPrPo ( $\tau_{\text{S}} = 9.76 \pm 0.03\text{ ns}$ )<sup>14</sup> and of TPP ( $\tau_{\text{S}} = 13.6\text{ ns}$ ),<sup>35</sup> indicating more efficient non-radiative decay processes than in the latter compounds. The radiative decay rate constant is readily calculated as  $k_{\text{F}} = \Phi_{\text{F}}/\tau_{\text{S}} = 3.1 \times 10^7\text{ s}^{-1}$  (Table 2), comparable to that of TPrPo and is *ca.* three-fold larger than that of TPP.<sup>31</sup> Of course this is consistent with the higher molar absorption coefficient (Strickler–Berg equation).

**Fig. 2** Absorption spectra of the porphycenes and their porphyrin counterparts. (a) TPPo and TPP; (b) PdTPPo and PdTPP; (c) CuTPPo and CuTPP. Note the factor  $\times 3$  in the 500–800 nm region.**Fig. 3** Fluorescence decay of TPPo in toluene,  $\lambda_{\text{exc}} = 375\text{ nm}$ ,  $\lambda_{\text{obs}} = 667\text{ nm}$ . Bottom panel: residuals of the fit to a monoexponential-decay function. Inset: fluorescence spectrum.

The singlet state energy is  $181 \pm 2\text{ kJ mol}^{-1}$ , slightly lower than that of TPP ( $184\text{ kJ mol}^{-1}$ ).<sup>31</sup> Oxygen quenches the singlet state with  $k_{\text{q}} = 5.5 \times 10^9\text{ M}^{-1}\text{ s}^{-1}$ . The triplet energy, determined by phosphorescence spectrophotometry in 1-iodopropane to take advantage of the heavy-atom effect, is  $124 \pm 2\text{ kJ mol}^{-1}$  (Fig. 4). It is essentially identical to that of TPrPo<sup>26</sup> and clearly lower than that of TPP ( $138\text{ kJ mol}^{-1}$ ).<sup>35</sup> Thus, bearing in mind that the singlet energies for both TPPo and TPP are very similar, the singlet–triplet energy gap is higher in TPPo than in TPP ( $57$  and  $46\text{ kJ mol}^{-1}$ , respectively).

Using laser-induced optoacoustic calorimetry, an enthalpy change upon triplet formation of  $\Phi_{\text{T}} \times E_{\text{T}} = 40.9\text{ kJ mol}^{-1}$  was found for TPPo (Fig. 5), which combined with the above triplet energy sets the value for the triplet quantum yield as  $\Phi_{\text{T}} = 0.33 \pm 0.04$ . This value is quite similar to that of TPrPo,  $\Phi_{\text{T}} = 0.4$ ,<sup>26</sup> but much lower than that of TPP,  $\Phi_{\text{T}} = 0.82$ .<sup>35</sup>

Interestingly, the intersystem-crossing rate constant, calculated as  $k_{\text{isc}} = \Phi_{\text{T}}/\tau_{\text{S}}$ , is similar for the three compounds (Table 2). Thus, it is mainly internal conversion that is responsible for the reduction of the fluorescence and intersystem-crossing quantum yields. In fact, we calculate  $\Phi_{\text{ic}} = 0.52$  and  $k_{\text{ic}} = 1.1 \times 10^8\text{ s}^{-1}$  for TPPo, five-fold higher than for TPrPo,  $\Phi_{\text{ic}} = 0.22$  ( $k_{\text{ic}} = 2.3 \times 10^7\text{ s}^{-1}$ ), and 30-fold higher than for TPP,  $\Phi_{\text{ic}} = 0.05$  ( $k_{\text{ic}} = 3.7 \times 10^6\text{ s}^{-1}$ ). The difference between the internal conversion rate constants for TPPo and TPP cannot be explained by the energy-gap law alone since their singlet energies are only slightly different ( $180$  and  $184\text{ kJ mol}^{-1}$ , respectively). On the other hand, efficient internal conversion is generally observed in non-rigid porphyrinoids since the lack of rigidity enables the molecule to reach the geometry that favours  $\text{S}_1$  deactivation without a significant energy barrier *i.e.*, involving an enhanced Franck–Condon factor for internal conversion.<sup>37–39</sup> It is thus conceivable that the introduction of four phenyl groups in porphycene further reduces the rigidity of this macrocycle. Additional mechanisms such as excited-state tautomerization followed by internal conversion and back proton transfer to the initial state might contribute as

**Table 2** Rate constants of fluorescence, internal conversion and intersystem-crossing of the excited singlet states of TPPo, TPrPo<sup>14,26</sup> and TPP<sup>31</sup> in toluene

Compound	$k_{\text{F}}/\text{s}^{-1}$	$k_{\text{ic}}/\text{s}^{-1}$	$k_{\text{isc}}/\text{s}^{-1}$
TPPo	$3.1 \times 10^7$	$1.1 \times 10^8$	$6.9 \times 10^7$
TPrPo	$3.9 \times 10^7$	$2.3 \times 10^7$	$4.1 \times 10^7$
TPP	$9.6 \times 10^6$	$3.7 \times 10^6$	$6.0 \times 10^7$

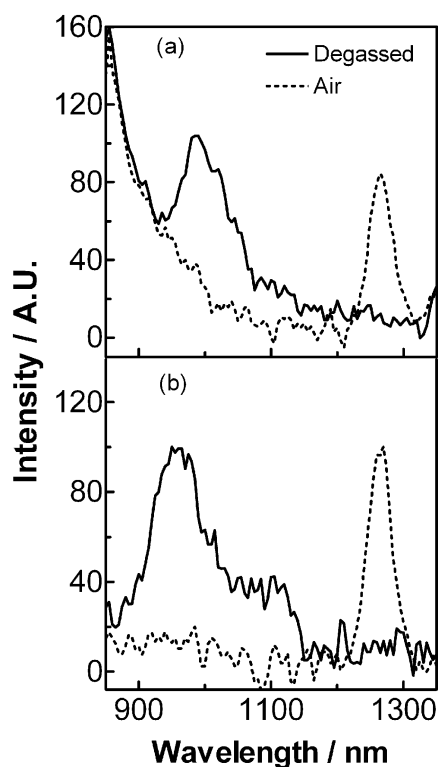


**Fig. 4** Near-IR emission spectra of (a) TPPo in 1-iodopropane and (b) PdTPPo in toluene. Phosphorescence in degassed solutions is replaced by  $O_2(^1\Delta_g)$  emission at 1270 nm when air is allowed into the cell.

well, suggesting a role of the N–H bonds as vibronic sinks.<sup>40</sup> Experiments are currently in progress to further understand this process.

The triplet state of TPPo has a lifetime of 51  $\mu$ s in toluene and 176  $\mu$ s in benzonitrile, much shorter than those of TPrPo ( $\tau_{T,TPPo} = 270 \mu$ s)<sup>41</sup> and especially of TPP ( $\tau_{T,TPP} = 1380 \mu$ s).<sup>35,42</sup> The triplet-minus-singlet absorption spectrum (Fig. 6) shows its maximum at 420 nm with differential absorption coefficient  $\Delta\epsilon_{T-S} = 11950 \text{ M}^{-1} \text{ cm}^{-1}$ . Monoexponential decay kinetics with the same lifetime were observed throughout the spectrum.

The triplet lifetime is long enough to produce a rich bimolecular photochemistry. Thus, energy transfer to molecular oxygen takes place with rate constant  $2.9 \times 10^9 \text{ M}^{-1} \text{ s}^{-1}$ , similar to that of TPrPo ( $2.9 \times 10^9 \text{ M}^{-1} \text{ s}^{-1}$ )<sup>41</sup> and TPP ( $2.1 \times 10^9 \text{ M}^{-1} \text{ s}^{-1}$ ).<sup>43</sup> Singlet oxygen is produced with  $\Phi_A = 0.23$  in toluene, a value comparable to that for other porphycenes, e.g. TPrPo ( $\Phi_A = 0.36$ ) or Po ( $\Phi_A = 0.34$ )<sup>26</sup> and much lower than

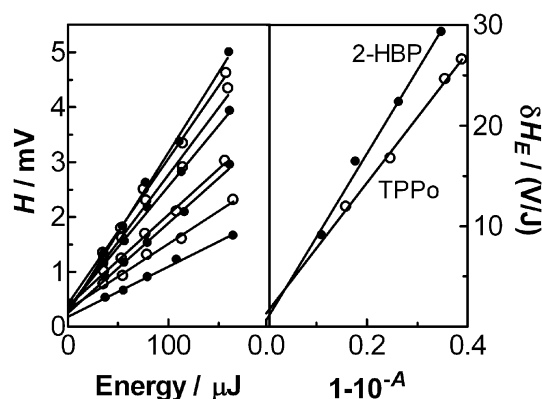


**Fig. 5** (a) Dependence of the optoacoustic wave amplitude on the fraction of light absorbed for argon-saturated toluene solutions of TPPo and 2-HBP.  $\lambda_{exc} = 337 \text{ nm}$ .

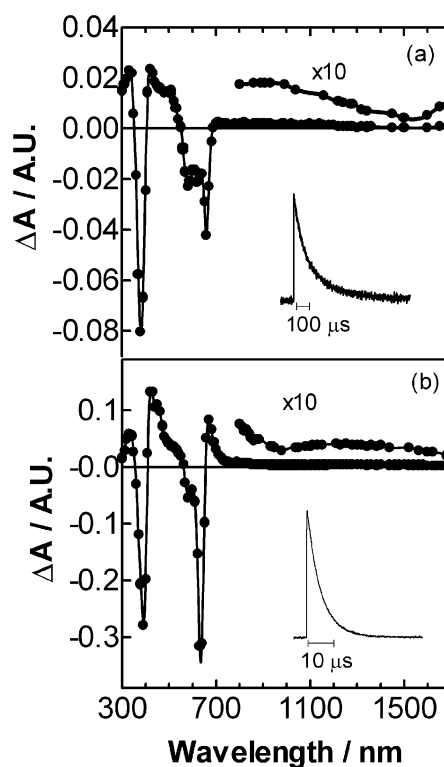


**Fig. 6** Triplet-minus-singlet absorption spectra of (a) TPPo and (b) PdTPPo in argon-saturated benzonitrile. Inset: transient decays at 420 nm. Monoexponential decay kinetics with the same lifetime were observed throughout the spectrum.

that for the porphyrin isomer TPP ( $\Phi_A = 0.68$ ).<sup>43</sup> Finally, while TPPo is very photostable, it is a moderate physical quencher of  $O_2(^1\Delta_g)$  in dichloromethane with  $k_q^s = 4.0 \times 10^7 \text{ M}^{-1} \text{ s}^{-1}$ , a value similar to that determined for TPP,  $k_q^s = 4.4 \times 10^7 \text{ M}^{-1} \text{ s}^{-1}$  in benzene.<sup>44</sup>

#### Palladium- and copper-complexes

The absorption spectra of PdTPPo and CuTPPo have both similarities and differences compared to TPPo (Fig. 2). While the Soret band position is virtually unchanged major differences are observed in the Q region: (i) the three Q-bands are reduced to two as a result of the increase in symmetry, (ii) the lowest-energy Q-band suffers a hypsochromic shift that reflects electron donation from the metal into the porphycene, thus raising their energy; (iii) finally, the presence of metals also leads to an increase in the absorption coefficient of the lowest energy Q-band, which is a further advantage for PDT treatments compared to the free base.

Compared to metalloporphyrins (Fig. 2), the Q-bands of metalloporphycenes show substantially higher intensities and bathochromic shifts (80 nm for PdTPPo relative to PdTPP and 74 nm for CuTPPo relative to CuTPP, which contrast with the 11 nm of TPPo relative to TPP) while the Soret bands are blue shifted. It would thus seem that electron donation from the metal ion to the porphycene's ring is not as important as in the case of porphyrins.

The ratio of intensities between the Q and Soret bands depends on the central metal ion and varies from 0.76, for CuTPPo, to 0.99, for PdTPPo. This ratio has been linked in metallo-octaethylporphycenes (OEPc) $M^{II}$  to the mixing of the d-orbitals of the metal with those of the porphycene-ring.<sup>23</sup> In this reference, the intensity ratio of the two bands ranges from 0.42 for (OEPc)Ni to 0.82 for (OEPc)Zn and is interpreted as an indication of minimal mixing in the case of the zinc complex. Assuming that this correlation holds for our aryl counterparts, we would conclude that the CuTPPo complex



has a higher degree of orbital mixing than the PdTPPo compound.

PdTPPo and CuTPPo do not show fluorescence, an analogous situation to that found for PdTPP ( $\Phi_F = 2 \times 10^{-4}$ )<sup>45</sup> and CuTPP ( $\Phi_F < 10^{-3}$ ).<sup>31</sup> This clearly reflects an enhancement of the intersystem-crossing probability owing to the paramagnetic (in the case of copper) and heavy-atom effects (both). In contrast, PdTPPo and CuTPPo show phosphorescence (Fig. 4) which allows us to locate their triplet energy at 126 and 120 kJ mol<sup>-1</sup>, respectively, well below that of PdTPP and CuTPP (173 and 160 kJ mol<sup>-1</sup>, respectively).<sup>46</sup> Taking the position of the lowest-energy Q-band as a rough estimation of the singlet energy, singlet–triplet splittings of 62 kJ mol<sup>-1</sup> are calculated for both PdTPPo and CuTPPo, *ca.* 20 kJ mol<sup>-1</sup> larger than for the porphyrin counterparts.

Combining the  $E_T$  values with the enthalpic changes measured by LIOAC,  $\Phi_T \cdot E_T = 98.3$  and 43.8 kJ mol<sup>-1</sup> for PdTPPo and CuTPPo, respectively, the triplet quantum yields are calculated as  $\Phi_T = 0.78 \pm 0.06$  for PdTPPo and  $\Phi_T = 0.37 \pm 0.05$  for CuTPPo. Clearly, the perturbation exerted by the central metal ion is more important for the case of palladium, which increases  $\Phi_T$  by a factor of 2.4. Interestingly, the triplet quantum yields of PdTPPo and CuTPPo are lower than those of PdTPP and CuTPP, which are nearly 1.<sup>31</sup> This is a likely consequence of the strong competing internal conversion, which is as the most efficient deactivation process for CuTPPo.

The triplet-minus-singlet absorption spectrum shows its maximum at 400 nm for both metal complexes, with differential absorption coefficients  $\Delta\epsilon_{T-S} = 7030$  M<sup>-1</sup> cm<sup>-1</sup> for PdTPPo and 2774 for CuTPPo. The triplet PdTPPo decayed with monoexponential kinetics with a lifetime of 4.4  $\mu$ s in toluene ( $\tau_T = 6.2$   $\mu$ s in benzonitrile) similar to that of PdTPPrPo ( $\tau_T = 5$   $\mu$ s)<sup>19</sup> and shorter than that of TPPo (Fig. 6). A similar trend in lifetime reduction is observed in the porphyrin series ( $\tau_T = 380$   $\mu$ s for PdTPP<sup>31,45</sup> and  $\tau_T = 1380$   $\mu$ s for TPP).<sup>31,35</sup> It is noteworthy that the triplet lifetime of CuTPPo is 700 ns in toluene, substantially shorter than that of TPPo and PdTPPo but clearly longer than that of CuTPP ( $\tau_T = 90$  ns).<sup>31,46</sup> While the paramagnetic Cu(II) ion clearly interacts with the macrocycle's  $\pi$ -system as in CuTPP,<sup>47,48</sup> the effect of this interaction is clearly less important in the porphyrines. This observation is consistent with the low perturbations observed as well in the absorption spectrum and in the intersystem-crossing rate constant.

Albeit the PdTPPo and CuTPPo triplet lifetimes are much shorter than that of TPPo, they are still long enough to be deactivated by oxygen. Energy transfer from <sup>3</sup>PdTPPo to oxygen takes place with a rate constant of  $1.8 \times 10^9$  M<sup>-1</sup> s<sup>-1</sup>, comparable to that of TPPo ( $k_q^{O_2} = 2.9 \times 10^9$  M<sup>-1</sup> s<sup>-1</sup>), and that of PdTPP ( $k_q^{O_2} = 2.5 \times 10^9$  M<sup>-1</sup> s<sup>-1</sup>).<sup>43</sup> The quantum yield of singlet oxygen production is 0.78 (both in toluene and dichloromethane) while for PdTPP  $\Phi_{\Delta} = 1$ .<sup>43</sup> PdTPPo is a moderate O<sub>2</sub>(<sup>1</sup> $\Delta_g$ ) quencher in dichloromethane with  $k_q^S = 3.2 \times 10^7$  M<sup>-1</sup> s<sup>-1</sup>.

For CuTPPo, energy transfer occurs with rate constant  $k_q^{O_2} = 2.0 \times 10^9$  M<sup>-1</sup> s<sup>-1</sup> and  $\Phi_{\Delta}$  depends strongly on the concentration of O<sub>2</sub> (Fig. 7). In general,  $\Phi_{\Delta}$  is determined by the product of three quantities: the quantum yield of triplet formation,  $\Phi_T$ , the efficiency of triplet trapping by oxygen,  $f_{T\Sigma}$ , defined as  $f_{T\Sigma} = k_q^{O_2} [O_2] / (1/\tau_T + k_q^{O_2} [O_2])$ , and the efficiency of energy transfer within the triplet–oxygen pairs,  $S_{\Delta}$ . Thus  $\Phi_{\Delta} = \Phi_T \times S_{\Delta} \times k_q^{O_2} [O_2] / (1/\tau_T + k_q^{O_2} [O_2])$  which can be linearized as  $1/\Phi_{\Delta} = (1/\Phi_T \times S_{\Delta}) \cdot (1 + 1/(k_q^{O_2} \times \tau_T \times [O_2]))$ . From the intercept and slope of the linear plot in Fig. 7, the limiting value of the singlet oxygen quantum yield,  $\Phi_{\Delta}^{\infty} = \Phi_T \times S_{\Delta} = 0.33$  is obtained, together with the triplet lifetime at zero oxygen concentration,  $\tau_T = 740$  ns. Assuming  $S_{\Delta} = 1$  as for PdTPPo,  $\Phi_T = 0.33$  is obtained for CuTPPo, in excellent agreement with the LIOAC data.

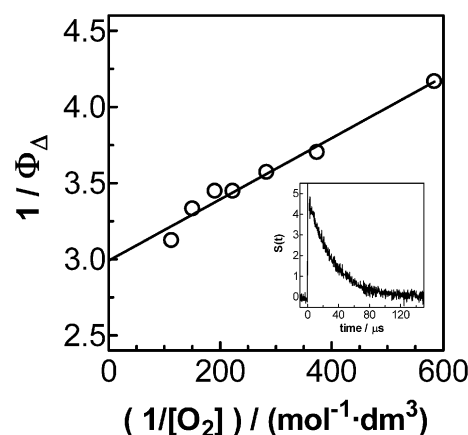


Fig. 7 Dependence of  $\Phi_{\Delta}$  on oxygen concentration for CuTPPo in dichloromethane. Inset: rise and decay of O<sub>2</sub>(<sup>1</sup> $\Delta_g$ ) phosphorescence at 1270 nm.

### Electrochemical properties

Cyclic voltammetry was used to determine reduction and oxidation potentials of the tetraphenylporphyrines. Unlike porphyrins, which show four different one-electron reductions, TPPo exhibited only two quasi-reversible one-electron reductions in both CH<sub>2</sub>Cl<sub>2</sub> and DMF (Fig. 8). This behaviour is consistent with that observed for alkyl-substituted porphyrines,<sup>50,51</sup> expanded porphyrines<sup>52</sup> and porphyrin isomers such as hemiporphyrine, corphyrine and isoporphyrine.<sup>53</sup> Two one-electron reduction steps were also observed for the reduction of PdTPPo and CuTPPo in CH<sub>2</sub>Cl<sub>2</sub> though the second peak was irreversible. The half-wave potentials are collected in Table 3. TPPo and its metal complexes are easier to reduce than their porphyrin counterparts,<sup>31</sup> a result that has been observed also for alkylporphyrines.<sup>50,51</sup>

The oxidation of TPPo in CH<sub>2</sub>Cl<sub>2</sub> shows an irreversible monoelectronic redox couple. Since the cathodic peak current increases with the scan rate and the plot of the peak current *vs.* the square root of the scan rate is not linear, an EC mechanism (electron transfer followed by a chemical reaction) is proposed to explain this process. In DMF the cathodic peaks completely disappear. The metalloporphyrines were oxidised in CH<sub>2</sub>Cl<sub>2</sub> in two one-electron steps: a first quasi-reversible oxidation followed by an irreversible one. Two one-electron reduction steps were also observed in CH<sub>2</sub>Cl<sub>2</sub>: a first reversible redox couple followed by an irreversible peak (Table 3). TPPo and its

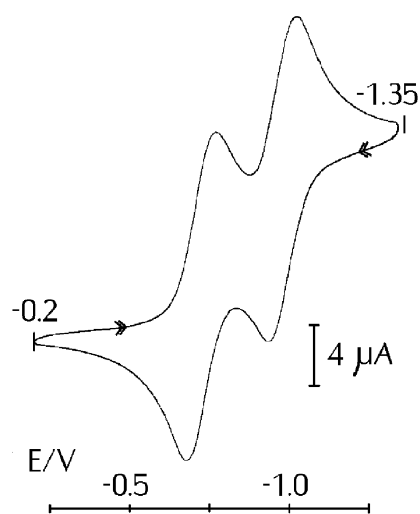


Fig. 8 Cyclic voltammogram for the reduction branch of TPPo ( $5 \times 10^{-4}$  M), 0.1 M TBAP in dichloromethane. Sweep speed: 100 mV s<sup>-1</sup>. (V *vs.* SCE).

**Table 3** Half-wave potentials of TPPo and its metallic complexes in CH<sub>2</sub>Cl<sub>2</sub> (in volt vs. SCE). Values for porphycene and tetrapropylporphycenes<sup>50,51</sup> and the isomeric porphyrins<sup>31,68,69</sup> are given for comparison

Compound	Oxidation		Reduction		$E_{\text{oxd1}} - E_{\text{red1}}$
	Second	First	First	Second	
TPPo	—	+1.08	−0.73	−0.98	1.81
PdTPPo	+1.17	+1.05	−0.73	−1.05	1.78
CuTPPo	+1.25	+1.02	−0.81	−1.06	1.83
Po	—	≈ +1.0	−0.73	−1.07	1.73
TPrPo	+1.44	+0.97	−0.90	−1.27	1.87
PdTPrPo	—	+0.88	−0.89	−1.28	1.77
CuTPrPo	+1.18	+0.88	−0.97	−1.32	1.85
TPP	+1.28	+0.95	−1.05	−1.47	2.00
PdTPP	—	+1.02	−1.00	—	2.02
CuTPP	+1.16	+0.90	−1.20	−1.68	2.10

metallocomplexes are more difficult to oxidise than their porphyrin counterparts and are thus more photostable under aerobic photoirradiation.<sup>31</sup>

For the series tetraphenyl- (TPPo), unsubstituted- (Po) and tetra-*n*-propyl- (TPrPo) porphycene, the sequence of the measured oxidation and reduction potentials reflects the electronic effects brought about by the substituents on the porphycene ring. Thus, the electron-withdrawing phenyl leads to a slightly easier reduction and a slightly more difficult oxidation compared to porphycene (Po),<sup>50,51</sup> while the electron-donating propyl does just the opposite. This observation parallels previous findings for the porphyrin family<sup>54–57</sup> as well as for other porphycenes.<sup>58</sup>

The potential difference between the first oxidation and the first reduction potentials ( $\Delta E$ ) is nearly constant in the tetraphenylporphycene series with  $\Delta E = 1.80 \pm 0.07$  eV, close to the value found for alkyl-substituted porphycenes ( $\Delta E = 1.85 \pm 0.04$  eV)<sup>20,50,51</sup> and smaller than those for porphyrins ( $\Delta E = 2.25 \pm 0.15$  eV).<sup>50,59</sup> This correlates to some extent with the lower energy of the Q-bands in porphycenes and has been linked by Bernard *et al.* to their lower symmetry.<sup>51</sup> The small variations among the redox potentials in TPPo and its Pd(II) and Cu(II)-complexes indicate that the first oxidative and reductive electron transfer processes involve ligand-centered orbitals.<sup>53,59,60</sup>

There is a correlation between the first reduction potentials of PdTPPo and CuTPPo and the electronegativity of the central ion. Thus, as in M(II)-tetrapropylporphycenes,<sup>51</sup> the

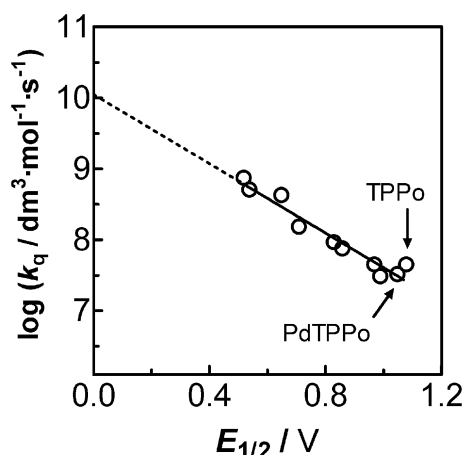


**Fig. 9** Correlation between the rate constant for quenching of O<sub>2</sub>(<sup>1</sup>Δ<sub>g</sub>) by the sensitizer and the oxidation half-wave potential and  $E_{1/2}^{\text{ox}}$  (data from ref. 49).

higher the electronegativity (EN) of the metal (EN (Pd) = 2.2 > EN (Cu) = 1.9)<sup>61</sup> the easier these porphycenes are reduced. This once more reflects that the energy of the LUMO orbital is perturbed by the central metal ion M(II).

Tanielian *et al.*<sup>44,62,63</sup> showed that for compounds such as chlorophylls and porphyrins a correlation exists between the rate constant of singlet oxygen quenching,  $k_q^S$ , and the oxidation potential. They concluded that the interaction of these compounds with singlet oxygen may involve formation of an exciplex, and that physical quenching may be envisaged as a spin-orbit-induced intersystem-crossing within it. Fig. 9 shows that TPPo and PdTPPo fall on Tanielian *et al.*'s linear plot, suggesting that singlet oxygen quenching by the porphycenes follows the same mechanism.

## 4. Conclusions

2,7,12,17-Tetraphenylporphycenes, especially TPPo and PdTPPo, show quite ideal photophysical properties for use in PDT. The introduction of phenyl rings, as expected, shifts the Q-bands to the red and enhances internal conversion, with the concomitant loss in fluorescence, triplet and singlet oxygen quantum yields compared to porphyrins and to alkyl-substituted porphycenes. The situation is alleviated by the introduction of metals. Thus, PdTPPo shows a very intense absorption in the red ( $\epsilon = 8.4 \times 10^4$  M<sup>−1</sup> cm<sup>−1</sup> at 632 nm, 20-fold larger than that for Photofrin®<sup>64,65</sup>) and a large <sup>1</sup>O<sub>2</sub> yield ( $\Phi_{\Delta} = 0.78$ ). The favourable photophysics, together with the ability to sensitise the photodynamic inactivation of several cell lines,<sup>7,8,11,12</sup> makes these compounds good candidates for PDT applications. Cells can be killed by either the so-called type-I mechanism, in which the photoexcited sensitizer oxidises essential cell components, or by the type-II mechanism, where singlet oxygen is formed. While the porphycenes are better oxidisers than the porphyrins in their ground state, the situation is reversed in the excited states on account of the lower triplet energies (Table 3). Hence one can reasonably expect cell photokilling by a type-I mechanism to be less important for porphycenes than for porphyrins. This seems to be the case in our studies on cultured cells.<sup>11</sup>

In the case of CuTPPo, its short triplet lifetime requires a high concentration of oxygen in the media for killing *via* a type-II mechanism or tight binding to a suitable biomolecule for killing *via* a type-I mechanism. This notwithstanding, some copper iminium salts of benzochlorin<sup>66,67</sup> have been found very effective in *in vivo* studies with transplanted experimental tumours.

## Acknowledgements

We wish to thank Dr J. L. Bourdelande (UAB) for assistance in early flash photolysis experiments, Dr G. Orellana (UAM) for early SPC experiments and Prof. S. E. Braslavsky for the near-IR phosphorescence spectra. N. R. and N. B. thank Fundació Patronat Institut Químic de Sarrià for a predoctoral fellowship. Financial support by the Spanish MCyT is gratefully acknowledged (grant no. SAF2002-04034-C02-02).

## References

- 1 E. Vogel, M. Köcher, H. Schmickler and J. Lex, *Angew. Chem., Int. Ed. Engl.*, 1986, **25**, 257.
- 2 G. Jori, *J. Photochem. Photobiol., A*, 1992, **62**, 371.
- 3 M. Guardiano, R. Biolo, G. Jori and K. Schaffner, *Cancer Lett.*, 1989, **44**, 1.
- 4 C. Milanesi, R. Biolo, G. Jori and K. Schaffner, *Lasers Med. Sci.*, 1991, **6**, 437.
- 5 C. Richert, J. M. Wessels, M. Müller, M. Kisters, T. Benninghaus and A. E. Goetz, *J. Med. Chem.*, 1994, **37**, 2797.
- 6 A. Aicher, K. Miller, E. Reich and R. Hautmann, *Urol. Res.*, 1994, **22**, 25.

- 7 A. Villanueva, M. Cañete, S. Nonell, J. I. Borrell, J. Teixidó and A. Juarraz, *Anti-Cancer Drug Des.*, 1996, **11**, 89.
- 8 M. Cañete, M. Lapeña, A. Juarraz, V. Vendrell, J. I. Borrell, J. Teixidó, S. Nonell and A. Villanueva, *Anti-Cancer Drug Des.*, 1997, **12**, 543.
- 9 S. Karrer, C. Abels, R.-M. Szeimies, W. Bäuml, M. Dellian, U. Hohenleutner, A. E. Goetz and M. Landthaler, *Arch. Dermatol. Res.*, 1997, **289**, 132.
- 10 S. Karrer, R.-M. Szeimies, A. Ebert, S. Fickweiler, C. Abels, W. Bäuml and M. Landthaler, *Lasers Med. Sci.*, 1997, **12**, 307.
- 11 M. Cañete, A. Ortiz, A. Juarraz, A. Villanueva, S. Nonell, J. I. Borrell, J. Teixidó and J. C. Stockert, *Anti-Cancer Drug Des.*, 2000, **15**, 143.
- 12 M. Cañete, C. Ortega, A. Gavalda, J. Cristóbal, A. Juarraz, S. Nonell, J. Teixidó, J. I. Borrell, A. Villanueva, S. Rello and J. C. Stockert, *Int. J. Oncol.*, 2004, **24**, 1221.
- 13 E. Vogel, M. Köcher, J. Lex and O. Ermer, *Isr. J. Chem.*, 1989, **29**, 257.
- 14 P. F. Aramendia, R. W. Redmond, S. Nonell, W. Schuster, S. E. Braslavsky, K. Schaffner and E. Vogel, *Photochem. Photobiol.*, 1986, **44**, 555.
- 15 A. D. Adler, F. R. Longo, F. Kampas and J. Kim, *J. Inorg. Nucl. Chem.*, 1970, **32**, 2443.
- 16 P. Sayer, M. Gouterman and C. R. Connell, *Acc. Chem. Res.*, 1982, **15**, 73.
- 17 C. J. Fowler, J. L. Sessler, V. Lynch, J. Waluk, A. Gebauer, J. Lex, A. Heger, F. Zuniga-y-Rivero and E. Vogel, *Chem.-Eur. J.*, 2002, **8**, 3485.
- 18 E. Vogel, M. Balci, K. Pramod, P. Koch, J. Lex and O. Ermer, *Angew. Chem., Int. Ed. Engl.*, 1987, **26**, 928.
- 19 M. Toporowicz, H. Ofir, H. Levanon, E. Vogel, M. Köcher, K. Pramod and R. W. Fessenden, *Photochem. Photobiol.*, 1989, **50**, 37.
- 20 M. W. Renner, A. Forman, W. Wu, C. K. Chang and J. Fajer, *J. Am. Chem. Soc.*, 1989, **111**, 8618.
- 21 J. Waluk, M. Müller, P. Swiderek, M. Köcher, E. Vogel, G. Hohlneicher and J. Michl, *J. Am. Chem. Soc.*, 1991, **113**, 5511.
- 22 E. Vogel, P. Koch, X. L. Hou, J. Lex, M. Lausmann, M. Kisters, M. A. Aukauloo, P. Richard and R. Guillard, *Angew. Chem., Int. Ed. Engl.*, 1993, **32**, 1600.
- 23 F. D'Souza, P. Bolas, M. A. Aukauloo, R. Guillard, M. Kisters, E. Vogel and K. M. Kadish, *J. Phys. Chem.*, 1994, **98**, 11885.
- 24 S. Nonell, N. Bou, J. I. Borrell, J. Teixidó, A. Villanueva, A. Juarraz and M. Cañete, *Tetrahedron Lett.*, 1995, **36**, 3405.
- 25 A. Gavalda, J. I. Borrell, J. Teixidó, S. Nonell, O. Arad, R. Grau, M. Cañete, A. Juarraz, A. Villanueva and J. C. Stockert, *J. Porphyrins Phthalocyanines*, 2001, **5**, 846.
- 26 S. Nonell, P. F. Aramendia, K. Heihoff, R. Martin-Negri and S. E. Braslavsky, *J. Phys. Chem.*, 1990, **94**, 5879.
- 27 S. E. Braslavsky and G. E. Heibel, *Chem. Rev.*, 1992, **92**, 1381.
- 28 R. V. Bensasson, C. R. Goldsmith, E. J. Land and T. G. Truscott, *Photochem. Photobiol.*, 1978, **28**, 277.
- 29 R. H. Compton, K. T. V. Grattan and T. Morrow, *J. Photochem.*, 1980, **14**, 61.
- 30 R. Bonnett, A. A. Charalambides, E. J. Land, R. S. Sinclair, D. Tait and T. G. Truscott, *J. Chem. Soc., Faraday Trans. 1*, 1980, **76**, 825.
- 31 J. R. Darwent, P. Douglas, A. Harriman, G. Porter and M. C. Richoux, *Coord. Chem. Rev.*, 1982, **44**, 83.
- 32 S. Nonell and S. E. Braslavsky, in *Singlet oxygen, UV-A and Ozone. Methods in Enzymology*, ed. L. Packer and H. Sies, Academic Press, San Diego, 2000, **vol. 319**, p. 37.
- 33 E. Oliveros, P. Suardi-Muraseco, T. Aminian-Saghafi, A. M. Braun and H.-J. Hansen, *Helv. Chim. Acta*, 1991, **74**, 79.
- 34 C. Martí, O. Jürgens, O. Cuenca, M. Casals and S. Nonell, *J. Photochem. Photobiol., A*, 1996, **97**, 11.
- 35 A. Harriman, *J. Chem. Soc., Faraday Trans.*, 1980, **76**, 1978.
- 36 G. J. Smith, *Photochem. Photobiol.*, 1985, **41**, 123.
- 37 S. Gentemann, C. J. Medforth, T. P. Forsyth, D. J. Nurco, K. M. Smith, J. Fajer and D. Holten, *J. Am. Chem. Soc.*, 1994, **116**, 7363.
- 38 S. Gentemann, C. J. Medforth, T. Ema, N. Y. Nelson, K. M. Smith, J. Fajer and D. Holten, *Chem. Phys. Lett.*, 1995, **245**, 441.
- 39 J. Dobkowski, V. Galievsky, A. Starukhin, E. Vogel and J. Waluk, *J. Phys. Chem. A*, 1998, **102**, 4966.
- 40 Y.-D. Wu and K. W. K. Chan, *J. Mol. Struct.*, 1997, **398–399**, 325.
- 41 S. Nonell, P. F. Aramendia, K. Heihoff, R. Martin-Negri and S. E. Braslavsky, *J. Phys. Chem.*, 1990, **94**, 5879.
- 42 J. R. Darwent, P. Douglas, A. Harriman, G. Porter and M. C. Richoux, *Coord. Chem. Rev.*, 1982, **44**, 83.
- 43 B. M. Dzharagov, K. I. Salokhiddinov, G. D. Egorova and G. P. Gurinovich, *Zh. Fiz. Khim.*, 1987, **61**, 2450.
- 44 C. Tanielian and C. Wolff, *Photochem. Photobiol.*, 1988, **78**, 277.
- 45 A. Harriman, *J. Chem. Soc., Faraday Trans. 2*, 1981, **77**, 1281.
- 46 A. Harriman, *J. Chem. Soc., Faraday Trans. 1*, 1981, **77**, 369.
- 47 S. C. Jeoung, D. Kim, D. W. Cho and M. Yoon, *J. Phys. Chem.*, 1996, **100**, 3075.
- 48 B. M. Dzharagov and G. P. Gurinovich, in *Vozbuzhdeniye Mol.*, ed. A. A. Krasnovsky, Izd. Nauka, Leningr. Otd., Leningrad, USSR, 1982, p. 59.
- 49 D. W. Clack and N. S. Hush, *J. Am. Chem. Soc.*, 1965, **87**, 4238.
- 50 J. P. Gisselbrecht, M. Gross, M. Köcher, M. Lausmann and E. Vogel, *J. Am. Chem. Soc.*, 1990, **112**, 8618.
- 51 C. Bernard, J. P. Gisselbrecht, M. Cross, E. Vogel and M. Lausmann, *Inorg. Chem.*, 1994, **33**, 2393.
- 52 C. Bernard, J. P. Gisselbrecht, M. Gross, N. Jux and E. Vogel, *J. Electroanal. Chem.*, 1995, **381**, 159.
- 53 J. P. Gisselbrecht, M. Gross, E. Vogel, P. Scholz, M. Bröring and J. L. Sessler, *J. Electroanal. Chem.*, 2001, **507**, 244.
- 54 A. Giraudeau, H. J. Callot, J. Jordan, I. Ezhar and M. Gross, *J. Am. Chem. Soc.*, 1979, **101**, 3857.
- 55 A. Giraudeau, H. J. Callot and M. Gross, *Inorg. Chem.*, 1979, **18**, 201.
- 56 F. D'Souza, A. Villard, E. Van Caemelbecke, M. Franzen, T. Boschi, P. Tagliatesta and K. M. Kadish, *Inorg. Chem.*, 1993, **32**, 4042.
- 57 K. M. Kadish, F. D'Souza, A. Villard, M. Autret, E. Van Caemelbecke, P. Bianco, A. Antonini and P. Tagliatesta, *Inorg. Chem.*, 1994, **33**, 5169.
- 58 F. D'Souza, P. L. Bolas, M. Kisters, L. Sambrotta, A. M. Aukauloo, R. Guillard and K. M. Kadish, *Inorg. Chem.*, 1996, **35**, 5743.
- 59 J.-H. Fuhrhop, K. M. Kadish and D. G. Davis, *J. Am. Chem. Soc.*, 1973, **95**, 5140.
- 60 K. M. Kadish, E. Van Caemelbecke, P. Bolas, F. D'Souza, E. Vogel, M. Kisters, C. J. Medforth and K. M. Smith, *Inorg. Chem.*, 1993, **32**, 4177.
- 61 N. N. Greenwood and A. Earnshaw, in *Chemistry of the elements*, Pergamon Press, Cambridge, UK, 1st edn., 1984, p. 1328.
- 62 C. Tanielian and L. Golder, *Photochem. Photobiol.*, 1981, **34**, 411.
- 63 C. Tanielian, G. Heinrich and A. Entezami, *J. Chem. Soc., Chem. Commun.*, 1988, 1197.
- 64 R. Pottier and T. G. Truscott, *Int. J. Radiat. Biol.*, 1986, **50**, 421.
- 65 J. G. Levy, *Semin. Oncol.*, 1994, **21**, 4.
- 66 G. M. Garbo, *J. Photochem. Photobiol., B*, 1996, **34**, 109.
- 67 J. A. Hampton, D. Skalkos, P. M. Taylor and S. H. Selman, *Photochem. Photobiol.*, 1993, **58**, 100.
- 68 R. H. Felton and H. Linschitz, *J. Am. Chem. Soc.*, 1966, **88**, 1113.
- 69 R. H. Felton, in *The Porphyrins*, ed. D. Dolphin, Academic Press, New York, 1978, p. 53.